29th Congress of the International Council of the Aeronautical Sciences
St. Petersburg, Russia; September 7-12, 2014

MESHLESS METHOD FOR SIMULATION OF COMPRESSIBLE REACTING FLOW

Jin Young Huh*, Kyu Hong Kim, Suk Young Jung*****
***Department of Mechanical & Aerospace Engineering, Seoul National University,**
****Department of Mechanical & Aerospace Engineering/Institute of Advanced Aerospace Technology, Seoul National University,**
*****Agency for Defense Development**

Keywords: *Meshless Method, Non-equilibrium Reacting Gas, Least Square Method, AUSMPW+, LU-SGS*

Abstract

This study aims to develop Meshless (or Gridless) method which can accurately capture shock waves in non-equilibrium reacting, compressible, inviscid flow where strong shocks are exist. Least square method was used for spatial discretization, and AUSMPW+ scheme, a robust and accurate scheme developed to be used for Finite Volume Method (FVM), was modified to be used for Meshless Method. In addition, minmod limiter was adopted to the developed Meshless method as a limiter for accurate calculation. LU-SGS method was also adopted for convergence.

Using the method developed from this study, numerical analyses for hypersonic blunt body with compressible reacting flow condition were carried out and the results compared with those obtained from Structured FVM using AUSMPW+ method for robustness, accuracy and convergence.

1 Introduction

Meshless method is a class of methods which behaves naturally and flexibly to cope with the flow near any complicated or moving geometry. The spatial discretization at any given point by Meshless method depends only on the information of neighboring points of the interested point so the forming a mesh is unnecessary. So, Meshless method has more less connectivity limitation of the mesh than conventional finite difference scheme using mesh system. Various Meshless methods have been studied and motivated by many former researchers. Among them, Smooth Particle Hydrodynamics method (SPH), the Element Free Galerkin method, Hp-clouds method, the Reproducing Kernel Particle method are well known methods [1]. In compressible aerodynamics, Upwind Finite Difference Scheme and Moving Least Square Method were developed by Sridar [2] and Katz [3] respectively and so on.

However, researches are focused primarily on subsonic/transonic flow until now. As shock capturing technique becomes important for high speed flows, some studies have been done for supersonic flows [4, 5]. It has been shown that strong shock capturing without numerical oscillation is fairly difficult from above researches. Much more intensified effort is needed for this kind of problems in hypersonic flow. As a means to address these shortcomings, Huh [6] developed Meshless method using AUSMPW+ scheme [7] with Multi-dimensional Limiting Process [8] for Euler flow. AUSMPW+ is a discretization scheme curing phenomena appearing in the application of AUSM-type schemes for hypersonic flows, such as pressure oscillation near wall and overshoot across strong shock. Multi-dimensional Limiting Process (MLP) is spatial high-order interpolation method which removes numerical oscillation in multi-dimension.

In this study, accurate and robust Meshless method is developed for capturing strong shock in non-equilibrium reacting flow. The scheme was applied to non-equilibrium Euler equation using least square method. AUSMPW+, robust scheme to capture strong shockwave, is applied to the Meshless method. Results were shown comparing with ones from finite volume method.

2 Meshless Method

2.1 Least Square Method

In the Meshless method, least square method based on Taylor series expansions has been used to get unknown derivative terms of PDE represented on equation (1).

Ignoring high order terms, the Taylor expansion from the point cloud center (x_0, y_0) is shown as

$$\varphi(x,y) = \varphi_0 + \Delta x \frac{\partial \varphi(x_0)}{\partial x} + \Delta y \frac{\partial \varphi(y_0)}{\partial y} + O(\Delta^2) \quad (1)$$

The least square method with weighted function may be expressed as follow

$$min \sum_{j=1}^{n} \omega_{0j} \left[\Delta\varphi_{0j} - \Delta x_{0j} \frac{\partial \varphi(x_0)}{\partial x} - \Delta y_{0j} \frac{\partial \varphi(y_0)}{\partial y} \right]^2 \quad (2)$$

$$\frac{\partial \varphi}{\partial x} \approx \sum_j a_{0j}(\varphi_j - \varphi_0) \quad (3)$$

$$\frac{\partial \varphi}{\partial y} \approx \sum_j b_{0j}(\varphi_j - \varphi_0) \quad (4)$$

For a 2-D case, values of the coefficients are calculated as follow

$$a_{0j} = \frac{\omega_{0j}\Delta x_{0j} \sum \omega \Delta y^2 - \omega_{0j}\Delta y_{0j} \sum \omega \Delta x \Delta y}{\sum \omega \Delta x^2 \sum \omega \Delta y^2 - (\sum \omega \Delta x \Delta y)^2} \quad (5)$$

$$b_{0j} = \frac{\omega_{0j}\Delta y_{0j} \sum \omega \Delta x^2 - \omega_{0j}\Delta x_{0j} \sum \omega \Delta x \Delta y}{\sum \omega \Delta x^2 \sum \omega \Delta y^2 - (\sum \omega \Delta x \Delta y)^2} \quad (6)$$

A simple inverse distance weighting function [9] is used to improve accuracy.

$$\omega_{0j} = \frac{1}{(\Delta x_{0j}^2 + \Delta y_{0j}^2)^{1/2}} \quad (7)$$

2.2 Euler Equation and AUSMPW+ for Meshless Method

Consider the 2-D Euler equation in strong conservation law form

$$\frac{\partial \omega}{\partial t} + \frac{\partial f}{\partial x} + \frac{\partial g}{\partial y} = 0 \quad (8)$$

$$\omega = \begin{bmatrix} \rho \\ \rho u \\ \rho v \\ \rho E \end{bmatrix},\ f = \begin{bmatrix} \rho u \\ \rho u^2 + P \\ \rho u v \\ \rho u E \end{bmatrix},\ g = \begin{bmatrix} \rho v \\ \rho u v \\ \rho v^2 + P \\ \rho v E \end{bmatrix} \quad (9)$$

In Eq. (9), E means a total energy and H means a total enthalpy as follow.

$$E = \frac{P}{(\gamma - 1)\rho} + \frac{1}{2}(u^2 + v^2),\ H = E + \frac{P}{\rho} \quad (10)$$

Eq. (8) can expressed as

$$\begin{aligned} &\frac{\partial \omega_i}{\partial t} + \sum_{j=1}^{n} a_{ij}\Delta f_{ij} + \sum_{j=1}^{n} b_{ij}\Delta g_{ij} \\ &= \frac{\partial \omega_i}{\partial t} + \sum_{j=1}^{n} \Delta F_{ij} = 0 \end{aligned} \quad (11)$$

where $F = af + bg$ is a directed flux along the metric weight vector (a, b). To improve accuracy and robustness, AUSMPW+ scheme [7] is applied to Meshless method, which use the midpoint flux at $\mathrm{j} + \frac{1}{2}$ instead of the flux at j as follow [2]

$$\sum_{j=1}^{n} \Delta F_{ij} = 2\sum_{j=1}^{n} \Delta F_{ij+\frac{1}{2}} = 2\sum_{j=1}^{n} \left(F_{ij+\frac{1}{2}} - F_{ij}\right) \quad (12)$$

In Eq. (12), $F_{ij+\frac{1}{2}}$ may be calculated from AUSMPW+ scheme.

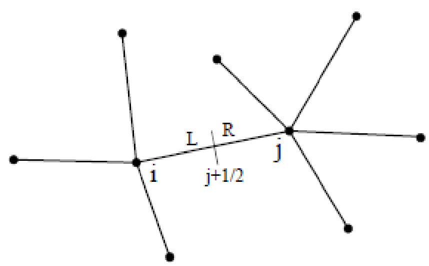

Fig. 1. Illustration of mid-point value on the edge connecting nodes i and j

The numerical flux of AUSMPW+ is given by

$$F_{\frac{1}{2}} = \bar{M}^{+}{}_{L} c_{\frac{1}{2}} \Phi_L + \bar{M}^{-}{}_{R} c_{\frac{1}{2}} \Phi_R + (P_L^{+} P_L + P_R^{-} P_R) \quad (13)$$

$\Phi = (\rho, \rho u, \rho H)^T$ and $\mathrm{P} = (0, p, 0)^T$. The subscripts 1/2 and (L,R) stand for a quantity at a midpoint on the edge of Fig. 1 and the left and right states across the edge, respectively. The Mach number at midpoint is defined as

$$m_{\frac{1}{2}} = \overline{M_L^+} + \overline{M_R^-} \tag{14}$$

when $\overline{M_L^+}$ and $\overline{M_R^-}$ are given as follow.

If $m_{\frac{1}{2}} = M_L^+ + M_R^- \geq 0$, then

$$\overline{M_L^+} = M_L^+ + M_R^-[(1-w)(1+f_R) - f_L] \tag{15}$$

$$\overline{M_R^-} = M_R^- w(1+f_R) \tag{16}$$

If $m_{\frac{1}{2}} = M_L^+ + M_R^- < 0$, then

$$\overline{M_L^+} = M_L^+ + w(1+f_L) \tag{17}$$

$$\overline{M_R^-} = M_R^- + M_L^+[(1-w)(1+f_L) - f_R] \tag{18}$$

with

$$w(P_L, P_R) = 1 - min\left(\frac{P_L}{P_R}, \frac{P_R}{P_L}\right)^3 \tag{19}$$

The pressure-based weight function is simplified to

$$f_{L,R} = \left(\frac{P_{L,R}}{P_s} - 1\right), P_s \neq 0 \tag{20}$$

where

$$P_s = P_L^+ P_L + P_R^- P_R \tag{21}$$

The split Mach number is defined by

$$M^{\pm} = \begin{cases} \pm\frac{1}{4}(M \pm 1)^2, & |M| \leq 1 \\ \frac{1}{2}(M \pm |M|), & |M| > 1 \end{cases} \tag{22}$$

$$P^{\pm} = \begin{cases} \frac{1}{4}(M \pm 1)^2(2 \mp M), & |M| \leq 1 \\ \frac{1}{2}(1 \pm sign(M)), & |M| > 1 \end{cases} \tag{23}$$

The Mach number of each side is

$$M_{L,R} = \frac{U_{L,R}}{c_{1/2}} \tag{24}$$

and the speed of sound($c_{1/2}$) is

$$c_{1/2} = \begin{cases} min\left(\frac{c^{*2}}{max(|U_L|, c^*)}\right), \frac{1}{2}(U_L + U_R) > 0 \\ min\left(\frac{c^{*2}}{max(|U_R|, c^*)}\right), \frac{1}{2}(U_L + U_R) < 0 \end{cases} \tag{25}$$

where

$$c^* = \sqrt{2(\gamma - 1)/(\gamma + 1)H_{normal}} \tag{26}$$

$$H_{normal} = \frac{1}{2}(H_L - \frac{1}{2}V_L^2 + H_R - \frac{1}{2}V_R^2) \tag{27}$$

2.3 Minmod Limiter for Meshless Method

To improve accuracy, TVD scheme is adopted to the Meshless method. In this study, minmod limiter [3] is used at AUSMPW+. The basic form of spatial interpolation is given by

$$\begin{aligned} \Phi_L &= \Phi_i + 0.5 * \phi_L * (\Phi_j - \Phi_i) \\ \Phi_R &= \Phi_j + 0.5 * \phi_R * (\Phi_i - \Phi_j) \end{aligned} \tag{28}$$

In order to apply to Meshless method, it is necessary to modify minmod limiter as follows. In Meshless method, ϕ is given by

$$\phi = max(0, min(1, r_k)), \tag{29}$$

where $k \in \{local\ point\ cloud\ of\ node\ i\ \&\ \theta_{kij}\ is\ max\}$,

$$r_k = \frac{s_{ik'}}{s_{ji}} = \frac{s_{ki}}{s_{ji}} cos(\theta_{kij}), \tag{30}$$

$$s_{ki} = \frac{\Phi_k - \Phi_i}{\|\vec{x_k} - \vec{x_i}\|} \tag{31}$$

Since there is no point on the opposite side of point j in the vicinity of point i in general point system, nearest point k to the opposite side is used to calculate r_k shown in Fig. 2.

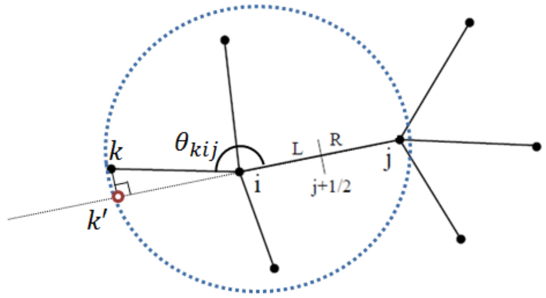

Fig. 2. Minmod limiter for Meshless method

3 Application of the Meshless Method to the Non-equilibrium Reacting Gas

For a non-equilibrium gas, all the species and vibrational energy equations must be included to describe the reaction process. Considering the species continuity and vibrational energy equations, the Euler equation (8) and the flow and flux vectors of the Euler equation become

$$\frac{\partial \omega}{\partial t} + \frac{\partial f}{\partial x} + \frac{\partial g}{\partial y} = S \qquad (32)$$

$$\omega = \begin{pmatrix} \rho \\ \rho u \\ \rho v \\ \rho e_t \\ \rho_i \\ \vdots \\ \sum_i \rho e_{vib,i} \end{pmatrix}, f = \begin{pmatrix} \rho u \\ \rho u^2 + p \\ \rho u v \\ (\rho e_t + p)u \\ \rho_i u \\ \vdots \\ \sum_i \rho e_{vib,i} u \end{pmatrix},$$
$$g = \begin{pmatrix} \rho v \\ \rho u v \\ \rho v^2 + p \\ (\rho e_t + p)v \\ \rho_i v \\ \vdots \\ \sum_i \rho e_{vib,i} v \end{pmatrix}, S = \begin{pmatrix} 0 \\ 0 \\ 0 \\ 0 \\ W_i \\ \vdots \\ \sum_i W_{vib,i} \end{pmatrix} \qquad (33)$$

S is the source term that includes W_i in the species continuity equations and $W_{vib,i}$ in the vibrational energy equation which are calculated according to Ref. [10] and [11].

4 LU-SGS for Meshless Method

Referring to the works of Yoon [12] and Chen [13], LU-SGS is adopted to Meshless Method. By applying Eq. (11) and (12), Euler equation (8) can be rewritten in a semi-discrete form as follows

$$\frac{\partial \omega_i^{n+1}}{\partial t} + 2\sum_{j=1}^{n}\left(F_{ij}^{n+1} - F_i^{n+1}\right) = S_i^n \qquad (34)$$

The flux function, F_{ij}^{n+1} may be linearized by setting

$$F_{ij}^{n+1}(\omega_i, \omega_j) \approx F_{ij}^n + A_{ij}^+(\omega_i)\delta\omega_i + A_{ij}^-(\omega_j)\delta\omega_j \qquad (35)$$

where n is the time level and matrices $A_{ij}^{\pm}$ are constructed as follow

$$A_{ij}^{\pm} = \frac{1}{2}(A_{ij} \pm \lambda_{ij} I) \qquad (36)$$

where

$$\lambda_{ij} \geq \max(|\lambda_A|) \qquad (37)$$

Here, λ_A represents eigenvalues of Jacobian matrix.

5 Numerical Result

In order to verify the Meshless method, numerical results for a hypersonic blunt body problem obtained using both Meshless method and finite volume method (FVM) with structured grid system were compared. The numerical schemes and flow conditions used are tabulated as Table 1.

Table 1. Schemes and flow conditions

Computational method	Meshless, structured FVM
Spatial discretization	AUSMPW+
Limiter	Minmod
Time integration	LU-SGS
Chemical Species	O,N,O_2,N_2,NO
Inflow Mach number	10
Inflow B.C.	Air (N_2 78%, O_2 22%), P=100 pa, T=300 K
Number of Points	5151

The Meshless method and FVM both used AUSMPW+. The point system for verification is shown in Fig. 3. Identically distributed grid points were applied to the both method. For structured FVM, additional information was used, which is connectivity of grid system. Fig. 4 shows the pressure field obtained by using the Meshless method with minmod limiter. Fig. 5, 6 show densities along stagnation line in frozen and non-equilibrium reacting flow respectively. As it can be seen from the figures, it has been observed that the results of the Meshless method is similar to those of FVM along stagnation line. Difference of shock location seems to come from that Meshless uses vertex based scheme while structured does cell-centered scheme. In addition, species density comparisons are shown in Fig. 7.

Lastly, convergence history of Meshless method and FVM are presented in Fig. 8. Despite the non-shock-aligned grid system on the downstream of the flow field, the figure shows the Meshless method has good convergence characteristics. Also, the Meshless method has as same accuracy and efficiency as conventional FVM using structured grid system.

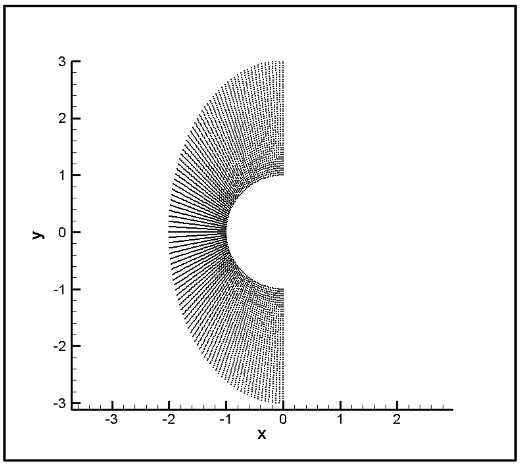

Fig. 3. Computational domain (5151 points).

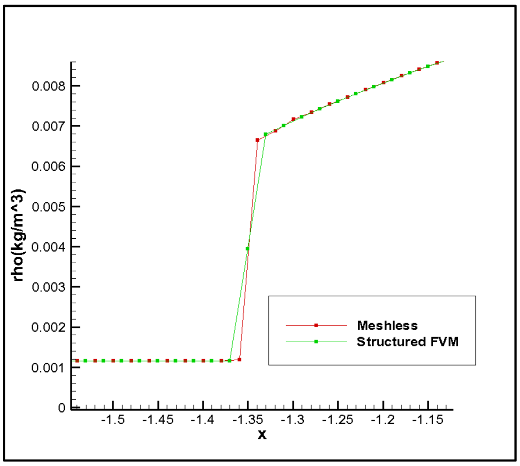

Fig. 6. Density comparison along stagnation line at non-equilibrium reacting flow

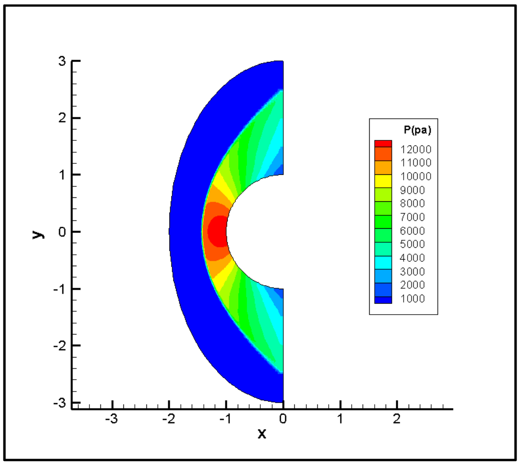

Fig. 4. Pressure contour computed using Meshless method with minmod limiter.

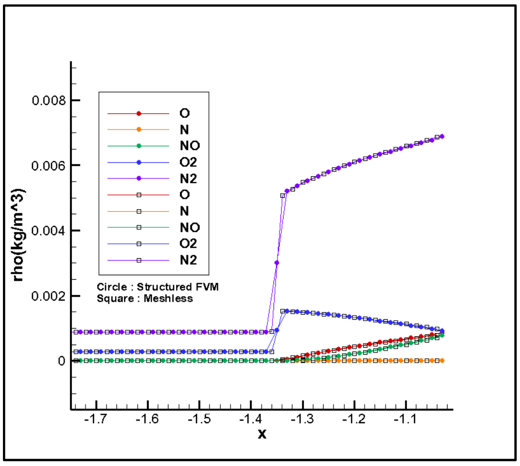

Fig. 7. Density comparisons of the chemical species along stagnation line

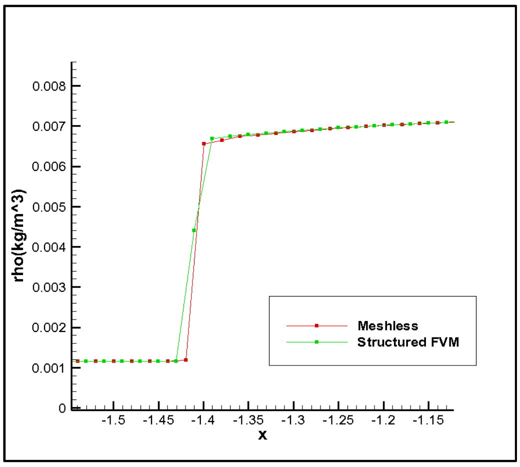

Fig. 5. Density comparison along stagnation line at frozen flow

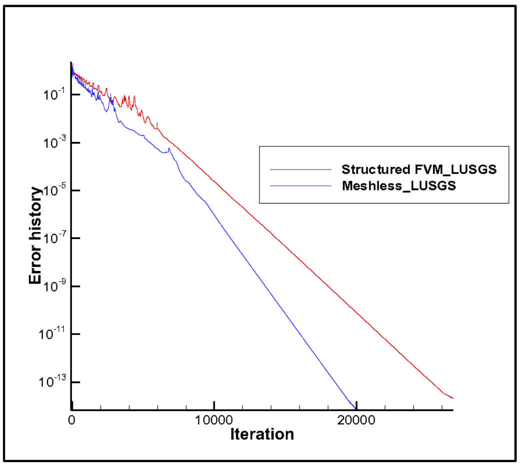

Fig. 8. Comparisons of convergence histories of implicit and explicit schemes

6 Conclusion

The purpose of this study is to develop Meshless method for accurately capturing shock waves in 2-D compressible non-equilibrium flow where strong shocks are present. A least square method was used for spatial discretization and AUSMPW+ scheme and LU-SGS was modified to be used for Meshless Method. According to the comparison analyses of the numerical results, Meshless method was confirmed to have similar robustness, accuracy and convergence compared to structured finite volume method.

References

[1] Liu G R. *Mesh Free Methods: Moving Beyond the Finite Element Method,* CRC Press, 2003.

[2] Sridar D and Balakrishnan N. An upwind finite difference scheme for meshless solvers, *J. Comput. Phys.*, Vol. 189, pp 1-29, 2003.

[3] Katz A and Jameson A. A Comparison of Various Meshless Schemes Within a Unified Algorithm, AIAA 2009-596, *47th AIAA Aerospace Sciences Meeting Including The New Horizons Forum and Aerospace Exposition*, Orlando, Florida, 2009.

[4] Tota P and Wang Z J. Meshfree Euler Solver using local Radial Basis Functions for inviscid Compressible Flows, *18th AIAA Computational Fluid Dynamics Conference*, Miami, Florida, 2007.

[5] Praveen C and Deshpande S M. Kinetic meshless method for compressible flows, *International Journal for Numerical Methods in Fluids*, Vol. 55, pp 1059-1089, 2007.

[6] Huh J, Kim K and Jung S. Meshless Method for Simulation of 2-D Compressible Flow, *The 2013 Asia-Pacific International Symposium on Aerospace Technology*, Takamatsu, Japan, 2013.

[7] Kim K, Kim C and Rho O. Methods for the Accurate Computations of Hypersonic Flows I. AUSMPW+ Scheme, *Journal of Computational Physics*, Vol.174, pp 38-80, 2001.

[8] Kim K and Kim C. Accurate, efficient and monotonic numerical methods for multi-dimensional compressible flows. Part II: Multidimensional limiting process, *J. Comput. Phys.,* Vol. 208, No. 2, pp 570-615, 2005.

[9] Mavriplis D J. Revisiting the least-squares procedure for gradient reconstruction on unstructured meshes, AIAA paper 2003-3986, *AIAA 16th Computational Fluid Dynamics Conference*, 2003.

[10] Park C and Yoon S. Fully Coupled Implicit Method for Thermochemical Nonequilibrium Air at Suborbital Flight Speed, *J. Spacecraft and Rockets*, Vol. 28, No. 1, pp 31-39, 1991.

[11] Candler G V. *The Computation of Weakly Ionized Hypersonic Flows in Thermo-Chemical Non equilibrium*, Ph.D. Thesis, Stanford Univ., 1988.

[12] Yoon S and Jameson A. Lower-Upper Symmetric-Gauss-Seidel Method for the Euler and Navier-Stokes Equations, *AIAA Journal*, Vol. 26, No. 9, pp 1025-1026, 1988.

[13] Chen H Q and Shu C. An Efficient Implicit Mesh-Free Method To Solve Two-Dimensional Compressible Euler Equations, *International Journal of Modern Physics C.,* Vol. 16, No. 3, pp 439-454, 2005.

Contact Author Email Address

Mailto:aerocfd1@snu.ac.kr

Copyright Statement